Behavior of CFRP strengthened RC multicell box girders under torsion

Abeer A. Majeed[*1], Abbas A. Allawi[2a], Kian H. Chai[3a] and Hameedon W. Wan Badaruzzam[4a]

[1]*Engineering Affairs Department, University of Baghdad, 17001 Baghdad, Iraq*
[2]*Department of Civil Engineering, University of Baghdad, 17001Baghdad, Iraq*
[3]*Department of Civil Engineering, Faculty of Engineering Building, University of Malaya, 50603 Kuala Lumpur, Malaysia*
[4]*Department of Civil and Structural Engineering, Faculty of Engineering, Universiti Kebangsaan Malaysia,*
43600 UKM Bangi, Selangor, Malaysia

Abstract.   The use of fiber reinforced polymer (FRP) for torsional strengthening of reinforced concrete (RC) single cell box beams has been analyzed considerably by researchers worldwide. However, little attention has been paid to torsional strengthening of multicell box girders in terms of both experimental and numerical research. This paper reports the experimental work in an overall investigation for torsional strengthening of multicell box section RC girders with externally-bonded Carbon Fiber Reinforced Polymer CFRP strips. Numerical work was carried out using non-linear finite element modeling (FEM). Good agreement in terms of torque-twist behavior, steel and CFRP reinforcement responses, and crack patterns was achieved. The unique failure modes of all the specimens were modeled correctly as well.

Keywords: concrete torsion; multicell box girder; carbon fiber reinforced polymer; strengthened girders; finite elements; nonlinear analysis

1. Introduction

The increase in service loads on structural elements requires the strength of these elements be upgraded to meet the new requirements. In certain situations, it may not be economically feasible to replace an outdated structure with a new one. Design and construction of a new structure to replace the existing one is not an attractive solution. In addition, the aging structures prompted many researchers to seek alternative materials and techniques to revive deteriorating structures. A potential solution is the use of new technologies to upgrade the deficient structures. In this context, strengthening with advanced composite materials, i.e., FRP systems in the form of external reinforcement is of great interest to the civil engineering community.

In utilising FRP composites for torsional strengthening of RC box girders, studies are aplenty for single box sections. It is to be noted that however, many concrete bridge superstructures consist of multi cells.

The multicell box girder bridge is aesthetically pleasing because the closed bottom slab and its shallow depth, especially when curved or sloped exterior webs cantilever overhangs are use, gives a compact appearance. From a structural point of view, the closed cross section of a multicell box is ideal to carry eccentric loads or torques introduced by skew supports. The high internal statically indeterminacy allows excellent transverse distribution of reactions and applied loads even without intermediate transverse diaphragms.

Numerous experimental and theoretical investigations have been carried out to capture this complex behavior of multi cellular structures. A summary of experimental and analytical studies on multicell box girder bridges has been given by Scordelis (1975). The Ministry of Transportation and Communications in Ontario (1974, 1975) has also reported extensively on analytical and experimental model and prototype investigations of post tensioned voided slab bridge structures. Experimental investigations on large-scale RC multicell box girder bridge models were conducted at the University of California, Berkeley, to obtain a better understanding of the actual behavior of a reinforced concrete prototype bridge. These tests show that reactions and internal forces can be predicted quite accurately by linear elastic analytical models for working stress loads, even after the bridge model has been subjected to higher overloads. However, the deflected state of the cracked RC structure and the response to overloads and ultimate failure loads cannot be predicted with a linear elastic analytical model. In early development by (Collins and Mitchell 1991, Hsu 1994), a set of equations are given for solving single cell torsion.

Later on, (Fu and Yang 1996) presented an algorithm to deal with the torsional problem for both reinforced concrete and prestressed concrete-box Girder Bridge superstructures with multiple cell sections. A computer program based on the Softened Truss Model Theory (STM) is developed and corresponding results are compared with previous theoretical and experimental work for single cell cases. It is considered that a more appropriate approach of strengthening should be developed for increased efficiency in strengthening multicell girders, (Chai *et al.* 2014)

∗Corresponding author, Lecturer
 E-mail: abeer.aqeel@uobaghdad.edu.iq
[a]Ph.D.

developed a new analytical method to predict the torsional capacity and behavior of RC multicell box girders strengthened with CFRP. Modification is done on the STM; the concrete torsional problem is solved by combining the equilibrium conditions, compatibility conditions and constitutive laws of materials by taking into account the confinement of concrete with CFRP strips, a specific algorithm was developed to predict the torsional behavior. The predictions using the Modified Softened Truss Model Theory MSTMT agreed reasonably with the experimental results, including both ascending and descending branches of the torque-twist curves. Applications of the developed method as an assessment tool to strengthen multicell box girders with CFRP and first analytical example that demonstrates the contribution of the CFRP materials on the torsional response is also included.

In order to have a better understanding of this behavior and add torsional strengthening to the archival data, a program of experimental research including single, double and triple cell box girders unstrengthened and strengthened with CFRP strips has been performed, the results of which are presented in this paper. A numerical study on RC multicell box girders with and without CFRP strengthening subjected to torsion is also presented. DIANA9.4.4 finite element software has been used in order to simulate girders in both linear and nonlinear range of response up to failure and the results are compared with the experiments. Here, the emphasis is on the ultimate torque and corresponding twist angle, history of torque-twist, the closeness of numerical and experimental results, and the strain in reinforcement and CFRP. The results as will be shown later are in good agreement with the experiments for the torque-twist behavior, elongation and strains of these girders.

2. Experimental program

2.1 Experimental design

Six relatively large-scale concrete box girders, 3000 mm long were constructed for this study. These girders are divided into two groups: the first group consists of three unstrengthened single, double and triple cell box cross section while the second group is of strengthened ones. Two of the girders were of single cell cross section with dimensions of 250 mm width and 350 mm depth while the other two girders were of two cells cross section, 500 mm width and 350 mm depth, and the other two girders were of three cells box section 750 mm width and 350 mm depth, all the reinforced specimens manufactured with constant concrete cover of 20 mm.

To avoid failure of the specimen at cracking, minimum steel reinforcement in both longitudinal and transverse directions was provided for torsion requirements. The total ratio of volume of stirrups and longitudinal reinforcement to the volume of the concrete was taken as 1.46% to avoid failure of the beams at torsional cracking load (MacGregor and Ghoneim 1995). This is an empirical relation based on experiments, for the limiting cover thickness, beyond which cover spalling would control the failure of the beam. When cover spalling controls failure of the beam, the effective
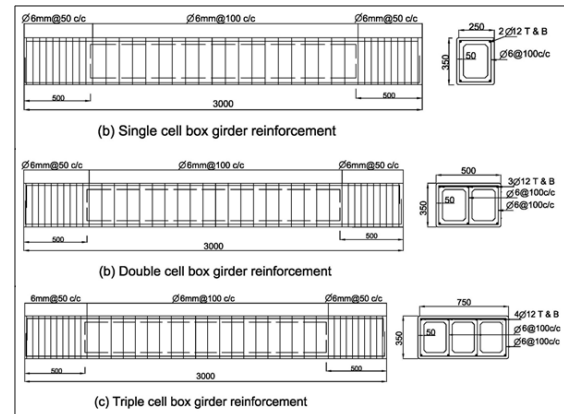

Fig. 1 Reinforcement details of the tested specimens

cross sectional area is calculated based on the centerline of the transverse reinforcement. In the present research program, all the reinforced specimens manufactured with constant concrete cover of 20 mm. The cover provided for the tested reinforced specimen satisfies the above mentioned statement and makes the concrete beyond the stirrups, of no value at ultimate. The reduction in effective cross sectional area of the reinforced concrete beam due to cover spalling leads to the reduction of ultimate strength in the reference specimens.

For the reinforced concrete beams with hollow cross section, the wall thickness was selected such that it will be enough to resist the axial thrust. This thickness was evaluated using the Modified Softened Truss Model Theory (MSTMT) for non-linear torsional analysis. Wall thickness of 50 mm was found to be sufficient for that. In addition, wall interior corners were strengthened by providing haunches as shown in Fig. 1.

In reinforced concrete beams subjected to torsion, cover spalling occurs due to excessive axial thrust on concrete at regions close to beam edges. Rahal and Collins (1996) suggested that spalling takes place if the thickness of the concrete cover exceeds 30% of A_c/P_c, where A_c and P_c are the area and perimeter of concrete cross section, respectively. Based on these considerations, all the girders were reinforced with 12 mm-diameter bars (605 MPa yield strength) in the longitudinal direction and closed stirrups in the transverse direction with 6 mm diameter (402 MPa yield strength) at 100 mm on center, in the tested zone.

In order to apply the torque at the ends of the girder, the cross section of the ends was solid rectangular; the rigid connection of tested girders with the stiff massive blocks at their ends corresponds to the actual condition of the connection with the columns and transverse beam at its ends. This boundary condition did not affect the strength of the girder, as the test girder supports insured that the girder rotates freely, without frictional resistance to the applied torque. So, the both edges of the girders were reinforced with stirrups of 6 mm diameter (402 MPa yield strength) at 50 mm on center. Fig. 1 shows geometrical details of girders and steel reinforcement provided in the test zone as well as in the end zones. A summary of the specimen details can be found in Table 1, along with the average concrete compressive strength of cylinder specimens. In the
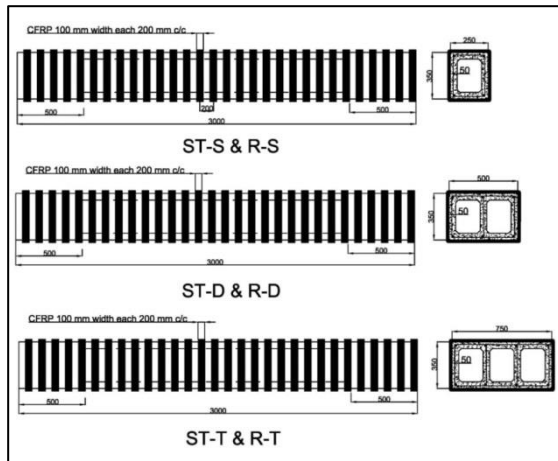
Fig. 2 CFRP Strengthening schemes of specimens

Table 1 Summary of specimen details and concrete test results

No.	Girder designation	Layout scheme/ Section type	Concrete Compressive Strength $(f_c')MPa$	Splitting Tensile Strength, (f_{ct}) MPa	Modulus of Elasticity, (E_c) MPa	Strip Spacing, mm
1	C-S	Control Single cell	45.0	2.72	31750	None
2	ST-S	Strengthened Single cell	45.0	2.52	27940	200
3	C-D	Control Double cell	43.0	2.72	31750	None
4	ST-D	Strengthened Double cell	43.0	2.52	27940	200
5	C-T	Control Triple cell	43.0	2.72	31750	None
6	ST-T	Strengthened Triple cell	43.0	2.52	27940	200

experimental study, CFRP sheets (Sika Wrap 231-C) were bonded to the specimens using the using the wet lay-up method by epoxy resin (Sikadur-330).
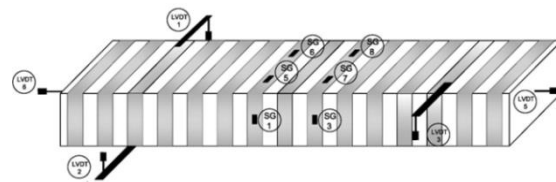
The manufacturer specified modulus and tensile strength of the fiber were 230 GPa and 4,900 MPa, respectively. CFRP strips with 100 mm of width were used in all the strengthened specimens. The strengthening configuration can be shown in Fig. 2.

2.2 Experimental test setup

The test setup is shown in Fig. 3. H-shape steel section stiffened by a tapered plate was used as cross beam to transfer the loading from the actuator of 1000 kN capacity to the two ends of lever arms, which were attached to the concrete girder and were capable of providing a maximum eccentricity of 1000 mm with respect to the longitudinal axis of the specimen. The reaction arm was supported by high strength threaded rods, which were anchored to the machine frame and can adjust the size of the supporting cover to be suitable for single and triple box girders. Two spherical seats were fashioned for the end supports of the beam specimen to avoid any axial restraints. Both ends were free to move longitudinally to allow for girder

Fig. 3 Photo of test setup

SG: strain gage, LVDT: Linear Variable Differential Transformer

Fig. 4 Positions and orientation of LVDTs and electrical strain gages in the tested triple cell specimen
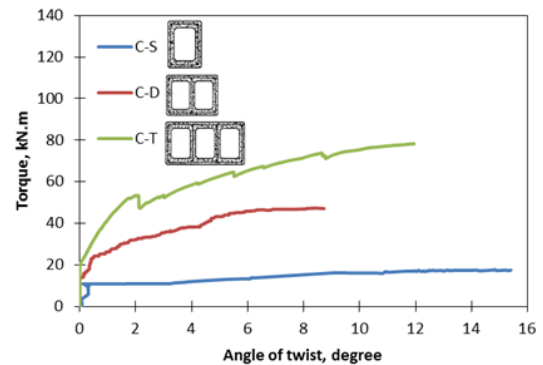

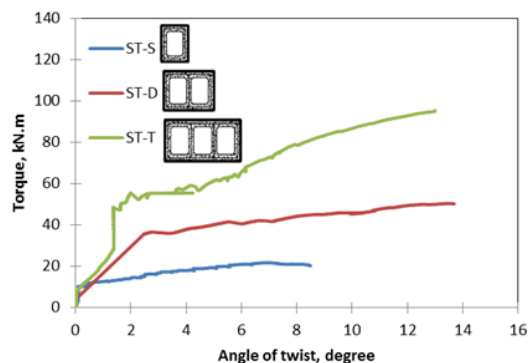Fig. 5 Torque-twist behavior for the unstrengthened specimens

Fig. 6 Torque-twist behavior for the strengthened specimens

elongation and allow twisting freely under the applied torque.

During testing, the main characteristics of the structural behavior of the girder were detected at every stage of loading. At each test, the first crack torque and the ultimate

Table 2 Cracking, ultimate torques, and corresponding twist angles of specimens

Specimens	Cracking Torque, kN.m	Twist at Cracking Torque (°)	Ultimate Torque, kN.m	Twist at Ultimate Torque (°)	% difference of T_u, assumption based on single cell box girder	Measured Elongation, mm	% of increase in elongation with respect to the reference girder, %
C-S	11.2	0.04	17.5	15.4	-	5.0	-
ST-S	12.2	0.07	21.5	7.2	-	20.0	300
C-D	33.0	0.06	47.2	8.8	43.8	23.0	360
ST-D	37.7	0.07	50.3	13.7	17.0	6.0	-
C-T	54.8	0.08	78.3	11.9	49.1	21.0	250
ST-T	57.5	2.1	95.3	13.0	47.8	20.0	233

torque were recorded. The strains were measured at the middle of the specimen in lateral rebars (Stirrups) and in CFRP in the transverse direction by using strain gauges, the angle of twist was calculated based on measurements of two installed LVDTs at the top and bottom of the specimen in the direction of twisting in both sides. The longitudinal displacements at specimen endsare measured by using LVDTs as shown in Fig. 4.

2.3 Test results

Figs. 5 and 6 show the torque versus twist angle of the girders throughout the loading regime up to failure obtained from the experiments of the unstrengthened and strengthened girders respectively.

Table 2 contains the ultimate torque-angle of twist, cracking torque-angle of twist and the difference percentage in ultimate torque base on single cell assumption for the tested specimens. CFRP rupture followed by excessive concrete crushing controlled the failure of the strengthened specimens ST-S, ST-D and ST-T. Comparison of test results with the unstrengthened specimens (C-S, C-D and C-T) reveals that the ultimate strength is increased. Specimens ST-S failed at an ultimate torque of 21.50 kN.m and angle of twist 7.20° with an increase in about 22.8% with respect to C-S, where ST-D failed at an ultimate torque of 50.3kN.m and of angle of twist 13.80° with an increase of about 6.6% with respect to C-D, this may be due to symmetrical geometry of the double cell box girder as compared with the single and triple cell box girders. Whereas specimen ST-T failed at ultimate torque of 95.30 kN.m with an angle of twist 13.0°in an increase of 21.7% with respect to C-T as shown in Figs. 5 and 6.

Specimens' first cracks were observed when the torsional moment reached approximately its 70% of maximum bearing capacity; the location of the first crack starts at the middle of the specimen. With the increasing load, the crack extended to the other sides of the specimen, eventually the crack connected to the four sides of specimen and the failure mode for all specimens was crushing of concrete. By analyzing the reference specimens, it is observed that the torsional stiffness of the specimens decreases with the appearance and propagation of cracks. With the widening of the cracks at mid-span, the steel is highly stressed and the structure has lost about 70% of its torsional stiffness.

The addition of CFRP strips resulted in a uniform, closely spaced cracks compared with the corresponding unstrengthened girders. The maximum torsional capacity for ST-D specimen and ST-T specimen are, 2.4 times and 4.7 times higher than torsional capacity of ST-S, respectively. The presence of CFRP inhibited the cracks from propagation and widening compared to the reference girders, so that the failure occurs in the unwrapped space between stirrups after the rupture of CFRP stirrup at the middle. The average inclination angle of spiral cracks with respect to the longitudinal axis was increased up to 65 degrees. This may be attributed to the presence of CFRP stirrups. It can be concluded that the torque based on single cell assumption is 43.8% and 17% lower than the total torque in case of double cell based on multicell assumption for the case of unstrengthened and strengthened girders respectively. For triple cells, the torque based on single cell assumption is 49.1% and 47.8% lower than the total torque
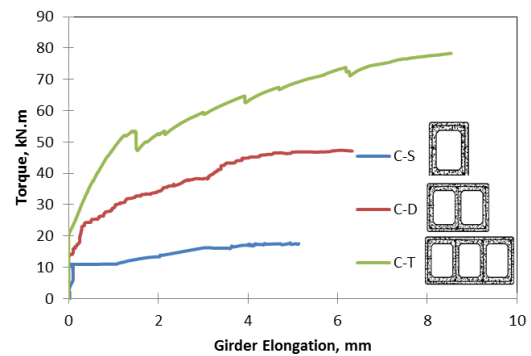

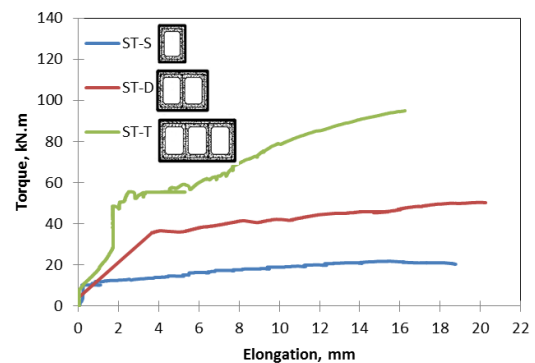Fig. 7 Torque-Elongation behavior for the unstrengthened specimen

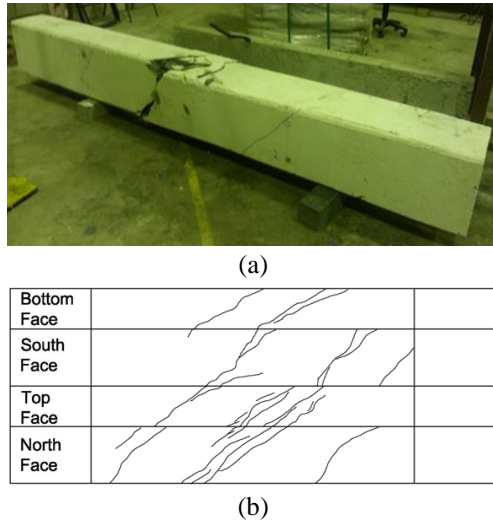Fig. 8 Torque-Elongation behavior for the strengthened specimens

(a)

(b)

Fig. 9 (a) Photo of tested unstrengthened single cell box girder C-S (b) Experimental crack pattern C-S
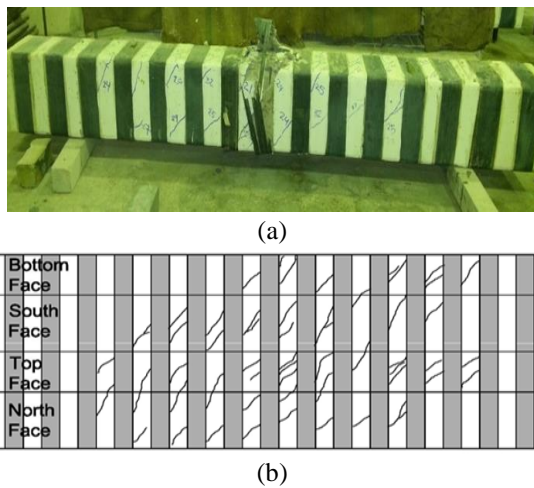

(a)

(b)

Fig. 10 (a) Photo of tested strengthened single cell box girder ST-S (b) Experimental crack pattern ST-S
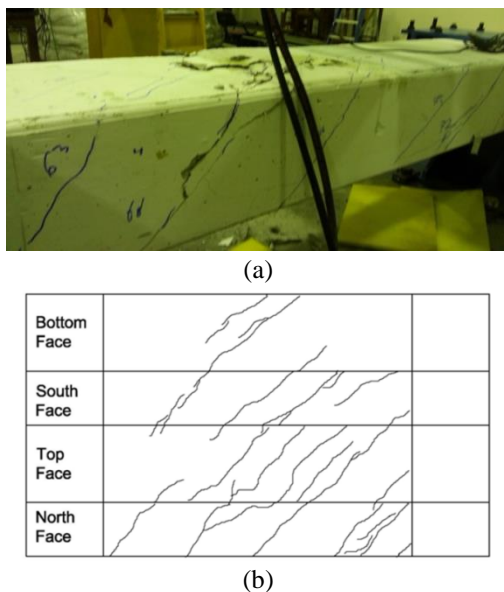

(a)

(b)

Fig. 11 (a) Photo of tested unstrengthened double cell box girder C-D (b) Experimental crack pattern C-D
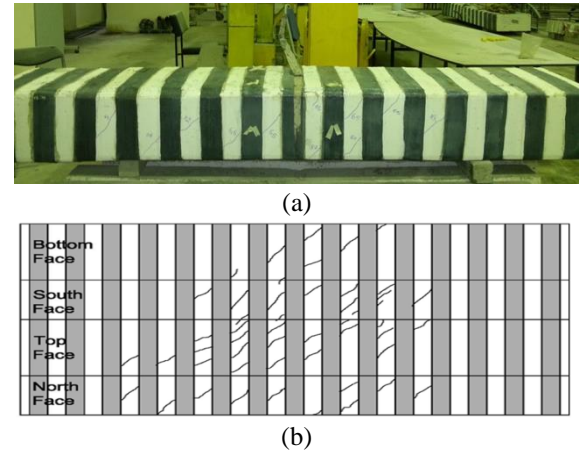

(a)

(b)

Fig. 12 (a) Photo of tested strengthened double cell box girder ST-D (b) Experimental crack pattern ST-D
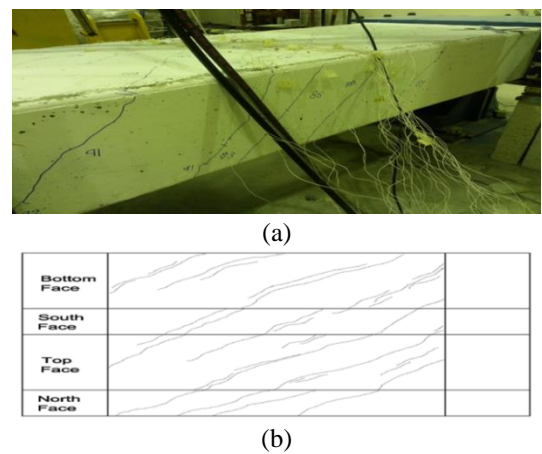

(a)

(b)

Fig. 13 (a) Photo of tested unstrengthened triple cell box girder C-T (b) Experimental crack pattern C-T
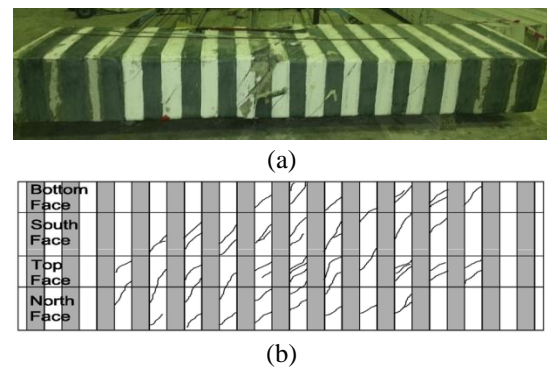

(a)

(b)

Fig. 14 (a) Photo of tested strengthened triple cell box girder ST-T(b) Experimental crack pattern of ST-T

based on multicell assumption for the case of unstrengthened and strengthened girders respectively.

Apparently, ST-S specimen has less ductility than other two specimens ST-D and ST-T after reaching peak point at 0.07° and 2.1° respectively. The angles of twist for the double and triple cell are more than 2 times higher than that for strengthened single cell. Figs. 7 and 8 show the elongation at center of supported edge of the tested unstrengthend and strengthened specimens respectively, the

maximum elongation for ST-S, ST-D and ST-T are relatively close, that means CFRP gives more confinement to the girder.

Figs. 9 to 14 show the crack details and failure modes for tested girders. For ST-S, ST-D, and ST-T specimens, it is very difficult to observe the cracks on the concrete part, which were covered by CFRP, so the crack pattern for the whole specimen can only be predicted. For the exposed concrete part, after finishing loading, the cracks are more dispersed than for C-S, C-D and C-T specimens, and the crack width is smaller.

As for the crack pattern, the complete loading, torsional moment did not seem to drop; big damage was not seen on the specimen. There are big damages at the exposed concrete part, which is located at middle of the specimen. Since the width (100 mm) of exposed concrete was between two CFRP strips, cracks of concrete became wider, finally got stripped and exfoliated by the torsional moment. As for CFRP, there was no stripping or rupture of CFRP observed during the completely loading test.

In addition, from the fact that cracking torsional moments of C-S, C-D and C-T specimens are near the peak point P, torsional moments at P can be treated as common cracking torsional moments of specimens. The torsional moments at P point for each specimen in Group (1), C-S, C-D and C-T specimen are 11.20 kN.m, 33.0 kN.m and 54.80 kN.m, respectively and for Group (2) ST-S, ST-D and ST-T are 12.20 kN.m, 37.70 and 57.50 kN.m, respectively. It is clear that cracking torsional moments of strengthened specimens are bigger. As for reinforced concrete specimens, concrete is confined by reinforcing steel bars (lateral ties), there is restraining effect on core concrete part, but it does not affect the covered concrete. Also, before cracks occurred, because strain is small, compared to the torsional resistance on the concrete section, torsional resistance shared by reinforcing bars can be ignored. Therefore, the cracking torsional moments are less than those of strengthened specimens. As for Group (2) specimens, when CFRP was introduced, the whole section is confined by CFRP, there is restraining effect even on the covering concrete part. Also, since CFRP covers the surface of the specimen, the arm length of torsional moment to specimen central axis become longer, so shared torsional resistance of CFRP becomes bigger accordingly. As a result, cracking torsional moment increases. The average inclination angle of spiral cracks with respect to the longitudinal axis was increased up to 45 degrees. This may be attributed to the presence of CFRP stirrups.

3. Numerical modeling

3.1 Materials Idealization

For reinforced concrete members with two dimensional torsion problems, it is necessary to do three dimensional analyses for strengthened members subjected to torsion. The finite element model is complicated and the analysis is difficult, one must consider fully when to apply each material model as the model must respond to the nonlinear behavior of reinforced concrete such as concrete cracking,

concrete plasticity, concrete crushing, and yielding of reinforcing steel, in addition to the elastic behavior of carbon fibers. To contribute to bridge the gap between research and practice in nonlinear finite element analysis, in this study, commercial finite element method computer program

TNO DIANA 9.4.4 (Manie and Schreppers, 2012) is used for the model analysis. A powerful FEM package is used to evaluate the effects of various nonlinear material models and their associated parameters on the torsional response of unstrengthened, strengthened structural concrete members. The 20-node hexahedral isoparametric brick element (**CHX60**) is used in the current study to model the concrete; the reinforcing bars are idealized as axial members embedded within the brick elements (Zeinkiwecz, 1971). Reinforcing bars are assumed capable of transmitting axial forces only. The stiffness matrix of steel bars is added to that of the concrete to obtain the global stiffness matrix of the brick element. CFRP sheet strips were modeled using eight-node quadrilateral isoparametric plane stress element (**CQ16M**). Due to the minimal thickness of the single layer used, it is suggested to consider the strips with a very low bending stiffness. It is also assumed that the out of plane forces are negligible, as loading and forces carried by the strips are mainly in plane. For these reasons, the aforementioned plane stress element is suitable for the model. (**CL12I - line, 3+3 nodes, 2-D**) interface elements were used to model the crack surface. The (**CL12I**) element is an interface element between two lines in a two-dimensional configuration.
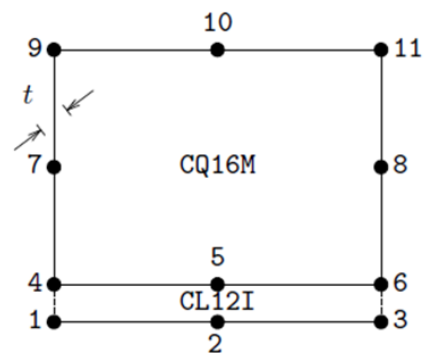

Fig. 15 (CL12I - line, 3+3 nodes, 2-D) Interface elements with shell (CQ16M) (Manie and Schreppers 2012)
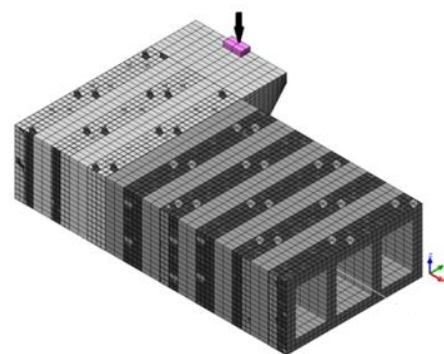

Fig. 16 Numerical modeling of triple strengthened box girder

3.2 Boundary and symmetry conditions

For the end support, a pivot point is placed at section center for the loaded end, Fig. 16. This point is fixed in the lateral and vertical directions (i.e., $\Delta x = \Delta y = 0$), but unrestrained in the longitudinal direction (Z-axis) to allow elongation of the girder under the applied torque. To counter localized concrete crushing at the pivot point (which did not appear in experimental tests), the concrete brick elements around the support are given linear elastic properties for concrete material.

At mid span, the beam cross section's surface was restrained against movement in the longitudinal, vertical and lateral directions (i.e., $\Delta x = \Delta y = \Delta z = 0$) at all end nodes to simulate the symmetry conditions at midspan and to allow the cross section to warp in the longitudinal direction.

3.3 Material models

Concrete cracking was based on the smeared crack approach. The constitutive model based on total strain is developed along the lines of the Modified Compression Field Theory, originally proposed by Vecchio and Collins (1986). The three dimensional extension to this theory is proposed by Selby and Vecchio (1993). The concrete compressive strength f_c', Young's modulus, and tensile strength for each model were based on tests results shown in (Table 1). The hardening and softening of concrete in compression was modeled using the Thorenfeldt function (Hii and Al-Mahaidi 2005). In tension, the behavior is based on a bilinear stress-strain relationship. The remaining shear stiffness of cracked concrete due to aggregate interlock is approximated with the shear retention factor β, which is the proportion of the elasticshear modulus.

An elastic bilinear work hardening model is adopted to simulate the uniaxial stress-strain behavior of reinforcing steel bars. Yielding of the reinforcement was based on the Von Mises yield criterion with strain hardening. The Young's Modulus stress-strain curves used were from the results of the tensile tests of reinforcing steel bars.

Tensile and compressive behavior of CFRP is like a fabric, tensile stress-strain relationship of CFRP is like elastic material, and it does not bear compression stress. Definition of yield strength of CFRP is difficult because CFRP is ruptured and cannot bear any tensile stress when the tensile stress of CFRP reaches its tensile strength. Young modulus is almost constant until tensile strength. Therefore, the CFRP is defined with Young's modulus $E_f = 2.30 \times 10^5$ MPa and tensile strength 4900 MPa in tensile field and with a very small Young's modulus in compressive field. CFRP is an anisotropic material; carbon fiber is arranged in one direction (transverse direction of specimen). Therefore, in other directions, model the CFRP is with a very small Young's modulus. The Poisson's ratio was assumed to be 0.3.

In FEM analysis, two methods are applied to simulate the mechanical behavior between the CFRP and concrete. One is that mesh of CFRP and concrete share the same nodes. The other one is that between the concrete and CFRP, a quadrilateral interface element is modeled.

3.4 Results of non-linear finite element modeling

The accuracy of FEM is determined by ensuring that the ultimate torque is reasonably predicted as compared with the experimental results, and the torque - twist and torque - elongation curves are close to the experimental curves, also the strains in the CFRP and reinforcement are checked. Crack pattern, strain, stress, deformed shape behavior of all models are also presented.

As a result of the finite element analysis, the patterns of cracking for the unstrengthened and strengthened specimens are shown in Figs. 17 to 22, respectively. The E_{knn} presented in the figures is the concrete crack strain. In the finite element models, spiral cracks at an inclination to the longitudinal axis formed on all four faces, are comparable to the cracks formed in tests. A small number of large, discrete spiral cracks were found in unstrengthened girders, while the rest of the strengthened specimens remained with relatively less cracked at the strengthened surfaces. In comparison, smaller and more uniformly distributed cracks were found in strengthened specimens. It can be noticed that CFRP strips prevent the cracks from propagation
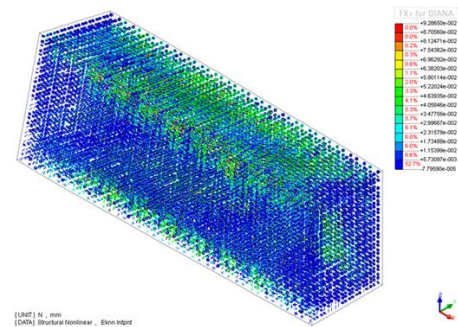

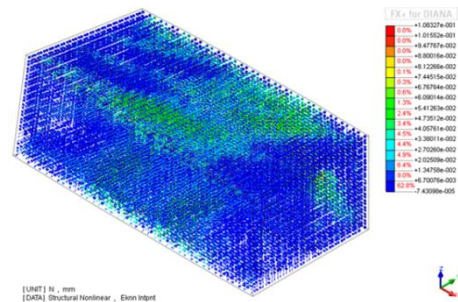Fig. 17 Numerical crack pattern of deformed C-S model

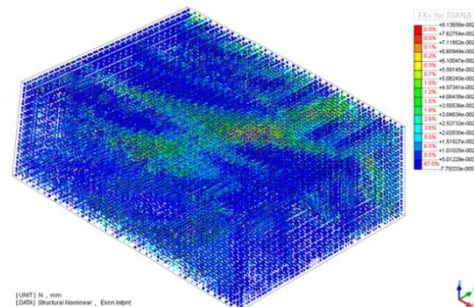Fig. 18 Numerical crack pattern of deformed C-D model

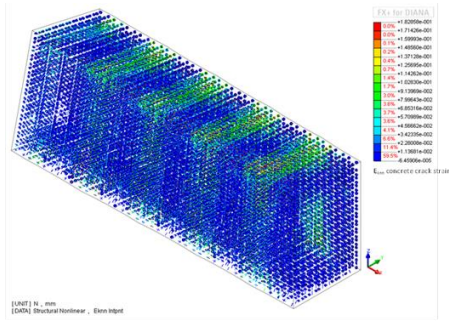Fig. 19 Numerical crack pattern of deformed C-T model

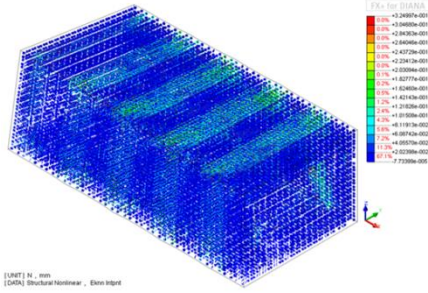Fig. 20 Numerical crack pattern of deformed ST-S model

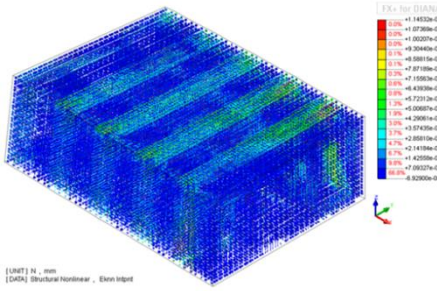Fig. 21 Numerical crack pattern of deformed ST-D model

Fig. 22 Numerical crack pattern of deformed ST-T model

through CFRP and enhance the model with less deformation.

It is clearly seen from Table 3, and (Figs. 23 and 24) that, the analysis results of the proposed model used in finite element analysis using DIANA V. 9.4.4 software shows very good agreement with the experimental skeleton of torque-twist and torque-elongation relationships, which reflect the strength and ductility enhancement provided by CFRP. In the finite element analysis using DIANA V. 9.4.4 software, loading on the studied specimens was induced by means of displacement control, this was found to be a powerful technique in predicting the post peak response of the tested girders. It has advantage over the load control method.

4. FIB Bulletin-14, 2001 design model

The full torsional strength of CFRP-strengthened RC beams can be analyzed by the design codes using the principle of superposition from both the steel and CFRP reinforcement. The proposed general form is shown in Eq. (1) (Hii and Al-Mahaidi 2007)
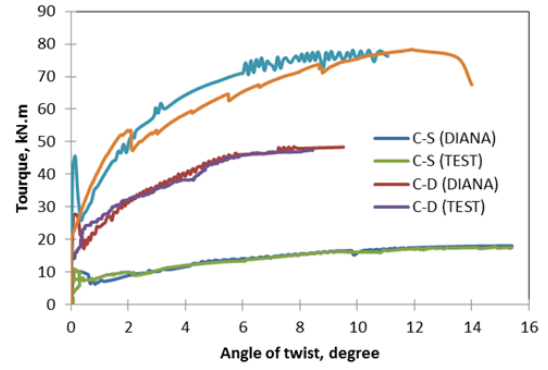

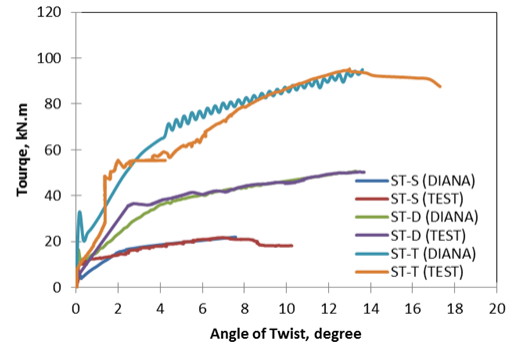Fig. 23 Torque-Twist behavior of unstrengthened specimens

Fig. 24 Torque-Twist behavior of strengthened specimens

$$T_n = T_{n,s} + T_{n,FRP} \tag{1}$$

Where T_n is the nominal torsional capacity of the FRP strengthened beam; $T_{n,s}$ is the nominal torsional capacity from steel reinforcement; and $T_{n,FRP}$ is the nominal torsional capacity from FRP reinforcement.
Hence

$$T_n = 2\,\frac{A_o A_{st} f_y}{S}\,cot\,\alpha +$$

$$2\,\varepsilon_{fd,e} E_f A_f S_f^{-1} A_c (cot\,\theta + tan\,\alpha)\,sin\,\alpha \tag{2}$$

A_o is the area enclosed to the perimeter of the shear flow zone according to ACI 318-05 (2005), A_{st} is the reinforcement area of the enclosed stirrups, f_y is the yield strength of the steel reinforcement, S is the spacing of the steel stirrups, A_f is the area of fiber strip/wrap, S_f is the centre to centre spacing of FRP strips, $\varepsilon_{fd,e}$ is design value of effective fiber strain, θ is angle between the principal fiber orientation and the longitudinal axis of member ; and α is the angle of crack to the longitudinal axis.

During the pre-critical response, the load control method may fail to predict the local maximum load, which usually occurs at the early stages after cracking. Displacements in the *X* direction to measure the girder elongation at centroid of the supported end are also presented and compared. Girder extension started at cracking torque. It was noted that the strengthened girders have higher axial displacement due to the restrain induced by CFRP when compared with corresponding unstrengthened girders at the same torque

Table 3 the maximum torsional capacity and increasing percentage

Specimen	T_{cr}, kN.m Test	T_u, kN.m Test	Increasing percentage T_{cr} %	Increasing percentage T_u %	T_{cr}, kN.m FEM, DIANA 9.4.4		T_u, kN.m FEM, DIANA 9.4.4		T_u, Eq. (2)	
					T_{cr}, kN.m	% of Test	T_u, kN.m	% of Test	T_u, kN.m	% of Test
C-S	11.2	17.5	-	-	11.50	94.3	17.8	101.7	14.8	84.6
C-D	33.0	47.2	-	-	34.50	104.5	48.3	102.4	32.44	68.8
C-T	54.8	78.3	-	-	58.50	106.7	78.5	100.2	50.0	63.8
ST-S	12.2	21.5	9.0	22.8	15.50	102.0	20.30	100.5	19.6	97
ST-D	37.7	50.3	14.3	6.6	35.50	94.0	50.0	99.50	45.8	91.3
ST-T	57.5	95.3	5.0	21.7	59.20	103.0	94.50	99.1	69.5	73

Table 4 Comparison of maximum stress and strain in stirrups and CFRP

Specimen	Test, Stirrups		FEM, Stirrups DIANA V. 9.4.4		Test, CFRP		FEM, CFRP DIANA V. 9.4.4	
	Stress, MPa	Strain, m/m	Stress, MPa	Strain, m/m	Stress, MPa	Strain, m/m	Stress, MPa	Strain, m/m
C-S	494	0.0025	400	0.0022	-	-	-	-
C-D	470	0.0024	400	0.0020	-	-	-	-
C-T	470	0.0023	435	0.0022	-	-	-	-
ST-S	427	0.0021	410	0.0021	621	0.0027	591	0.0025
ST-D	330	0.0016	378	0.0012	950	0.0043	1088	0.0047
ST-T	488	0.0024	492	0.0025	827	0.0036	904	0.0040

level. Results of maximum stresses at the center of the vertical side of lateral reinforcement and CFRP at ultimate torque for the tested girders are given and compared in Table 4.

For the unstrengthened specimens, the analytical results match test results well. In the finite element analysis model, reinforcing steel bars are modeled as embedded reinforcement elements. Strains of reinforcing bars are computed from the displacement field of the solid elements for concrete, and because the crack of concrete is modeled as smeared cracking model, when crack occurs, this model cannot estimate the practical cracks of specimens well.

Also, most of the ultimate torque predictions and strains in the CFRP for the strengthened specimens, using FEM model, are lower as compared to the values obtained through the tests. As discussed by Teng and Chen (2001), the crack propagation will be halted at the CFRP location, resulting in a non-uniform stress distribution across the CFRP strip due to inability of FRP composites to redistribute stresses. This non-uniformity of stress distribution and lack of ductility means that the failure process will start once the most highly stressed point in the CFRP reaches its ultimate tensile strength. The brittleness of CFRP composites is a fundamental source of difference in behavior between steel and CFRP reinforcement. Also, it should be noted that when cracks occurred and widened, the CFRP is more highly stressed.

The design model was based on Modified Softened Truss Model Theory for torsion (MSTMT) to obtain the full torsional behavior of RC multi-cell box girders strengthened with CFRP sheets Abeer *et al.* (2013). This study is an attempt to extend and modify the STM

algorithm to be applicable to nonlinear torsional analysis that takes into consideration the effect of CFRP sheet confinement to concrete. FIB Bullutin-14 2001 method for torshional analysis was also compared to a database compiled from current experimental data (Chai *et al.* 2014). From table 3 it can be concluded that recommendation of ACI318-08 and FIB-14 (2001) underestimate the torsional capacity of the tested specimens.

5. Conclusions

This work was undertaken to determine the effect of strengthening of multicell RC box girders with externally bonded CFPR strips and to show how to simulate the nonlinear torsion response in concrete members with and without CFRP. Modeling method that can be used for evaluation of the response and the load carrying capacity of multicell R.C concrete bridges were worked out and verified by nonlinear analyses of tests. In general, the finite element analyses of the tests could describe the overall behavior, failure mode, crack pattern, maximum load, and torsion-angle of twist relationships quite well. According to the comparison of test results with the proposed FEM, the following conclusions are made:

1. The assumption of single cell model cannot predict the torsional response of multicell girder accurately. Hence, the torque based on single cell assumption is (43.8%) lower than the total torque in case of double cell based on multicell assumption. For triple cells, the torque based on single cell assumption is (49.1%) lower than the total torque based on multi-cell assumption for the case of unstrengthened girders. The percentage of difference for strengthened single and triple cell specimens were recorded 17% and 47.8% less than the total torque based on multicell assumption respectively.

2. Strengthening with CFRP strips exhibit an increase in the ultimate strength. This increase reach up to 22.8%, 6.6% and 21.7% for specimens having single, double and triple cells respectively.

3. The strengthening of girders in torsion with external CFRP strips has an insignificant effect on restraining the strengthened girders from longitudinal elongation; the increasing percentage was ranged from 250-360%.

4. The three-dimensional finite element model used in the present work including both effects of confinement and expansion due to Poisson's ratio is able to simulate

the behavior of beams strengthened for torsion resistance.

5. Comparisons of the FEM results with experimental data show that the maximum differences from the experimental results are 6% and 2% as compared for cracking and ultimate torque, respectively.

6. The proposed confined concrete model including expansion effect has proved to be capable of providing good estimates of strength and deformations of concrete elements subjected to multiaxial compressive stresses and improved the accuracy close to ultimate values.

7. The proposed strengthened reinforced concrete model including interface element has proved to be capable of providing good estimates of strains and stresses in CFRP strips.

8. The predicted strains in CFRP for the strengthened girders obtained from FEM model is lower as compared to the experimental values since concrete crack modeling is based on the smeared crack approach in the model.

9. The potential of nonlinear finite element analysis to reveal higher load-carrying capacities and improved understanding of the mechanical behavior of concrete structures, which has been shown in many research projects.

10. The only torsional design available method for reinforced concrete members strengthened with CFRP recommended procedure of FIB-14 (2001) was found to be generally conservative. Further refinement is needed for guidelines to make them suitable as a design method for torsional strengthening.

Acknowledgments

References

Abeer, A.M., Allawi, A.A. and Chai, H.K. (2013), "Theoretical study on torsional strengthening of multi-cell RC box girders", *World Acad. Sci. Eng. Tech. Int. J. Civil Envir. Struct. Constr. Arch. Eng.*, **7**(2), 115-122.

Chai, H.K., Majeed, A.A. and Allawi, A.A. (2015), "Torsional analysis of multicell concrete box girders strengthened with CFRP using a modified softened truss model", *J. Bridge Eng.*, ASCE, **20**(8), B4014001.

Chalioris, C.E. (2008), "Torsional strengthening of rectangular and flanged beams using carbon fibre reinforced polymers, experimental study", *Constr. Build. Mater.*, **22**(1), 21-29.

Collins, M.P. and Mitchell, D. (1991), *Prestressed Concrete Structures*, Prentice Hall, Englewood Cliffs, New Jersey.

FIB (2001), Externally Bonded FRP Reinforcement for RC Structures.FIB Bulletin 14, FIB-International Federation for Structural Concrete, Lausanne.

Fu, C. and Yang, D. (1996), "Designs of concrete bridges with multiple box cells due to torsion using softened truss model", *ACI Struct. J.*, **94**(6), 696-702.

Hii, A.K.Y. and Al-Mahaidi, R. (2006), "An experimental and numerical investigation on torsional strengthening of solid and box-section RC beams using CFRP laminates", *Compos. Struct.*, **75**, 213-221.

Hsu, T.T.C. (1991b), "Nonlinear analysis of concrete torsional members", *Struct. J. Am. Concrete Inst.*, **88**(6), 674-682.

MacGregor, J.M. and Ghoneim, M.G. (1995), "Design for torsion", *ACI Struct. J.*, **92**(2), 211-218.

Majeed, A.A. (2013), "Torsional resistance of reinforced concrete multi-cell box girders strengthend with CFRP", Thesis Dept. of Civil Engineering, College of Engineering, Univ. of Baghdad, Baghdad, Iraq.

Manie, J. and Schreppers, G. (2012), *DIANA Finite Element Analysis-User's Manual, Release 9.4.4*, TNO DIANA BV Delftech park 19a, 2628 XJ Delft, The Netherlands.

Rahal, K.N. and Collins, M.P. (1996), "Simple model for predicting torsional strength of reinforced and prestressed concrete sections", *ACI Struct. J.*, **93**(6), 658-666.

Scordelis, A.C. (1975), *Analytical and Experimental Studies of Multi-Cell Concrete Box Girder Bridges*, Bulletin of the International Association for Shclls and Spatial Structures, Madrid. No. 58.

Selby, R.G. and Vecchio, F.J. (1993), "Three-Dimensional Constitutive Relations for Reinforced Concrete", Tech. Rep., 93-02, Univ. Toronto, Dept. Civil Eng., Toronta, Canada.

Teng, J.G., Chen, J.F., Smith, S.T. and Lam, L. (2001), *FRP: Strengthened RC Structures*, Wiley, Technology & Engineering.

Vecchio, F.J. and Collins, M.P. (1986), "The modified compression field theory for reinforced concrete elements subjected to shear", *J. Am. Concrete Inst., Proc.*, **83**(2) 219-231.

Zienkiewicz, O.C. (1971), "Incremental displacement in non-linear analysis", *Int. J. Numer. Meth. Eng.*, **3**, 587-592.

PL